

Simulation of Rotation Behavior of a 14-12 Spherical Motor

Kazuki Adachi, Akio Gofuku

Graduate School of Natural Science and Technology
Okayama University
Okayama, Japan
fukuchan@sys.okayama-u.ac.jp

Tomoaki Yano

Research Institute of Fundamental Technology for Next
Generation
Kinki University
Higashi-Hiroshima, Japan

Abstract—A spherical motor called as the 14-12 spherical motor has been developed. The motor rotates around two kinds of rotation axes and totally six rotation axes. The previous studies presented its structure, working principle of rotation by five-phase alternative currents (ACs), and experimental evaluation results of rotation torque and cogging torque around rotation axes. A numerical simulation is a strong tool to estimate dynamic rotation behavior of the motor and to investigate optimum values of design parameters. This study constructs a simulation model of the 14-12 spherical motor and conducts several simulations of rotation behavior by a software package to simulate magnetic field coupling with motion.

Keywords—spherical motor; rotation behavior; computer simulation; simulation model; rotation speed

I. INTRODUCTION

A spherical motor has multiple rotation axes. By the characteristic feature, a joint of a robot arm with three degrees of freedom can be controlled by only one spherical motor and a vehicle driven by a spherical motor can realize holonomic movement.

Recently, spherical motors driven by magnetic forces were widely studied and developed[1-3]. The authors developed a spherical motor[4] that rotates in any direction with small rotation angle error and confirmed its applicability to stirrers[5] and holonomic vehicles[6]. A spherical motor what the authors call 14-12 spherical motor[7] is also developed from a group of spherical motors that can have large rotation torques. The 14-12 spherical motor has two kinds of rotation axes and totally six rotation axes. The basic rotation performances such as maximum rotation speed, maximum rotation torque, cogging torque, etc. are evaluated by experiments[8, 9].

The rotation performances of spherical motors are usually evaluated by experiments and/or numerical simulations based on simple models. Experiments have difficulties in evaluating dynamic behaviors of spherical motors such as the change of rotation torque depending on rotation angle. Utilization of simple models in numerical simulations has limited applicability in an optimum design of a spherical motor. Recently, several software packages to simulate dynamic behaviors of motors become to be available. These software packages are strong tools to evaluate detailed rotation

performances of spherical motors and to investigate optimum values of design parameters.

This study develops a structure model of the 14-12 spherical motor based on its design parameters and simulates its dynamic behavior by a commercial software package. In the following, this paper describes the 14-12 spherical motor, its structure model, and simulation results of rotation around two kinds of rotation axes.

II. 14-12 SPHERICAL MOTOR

A. Structure

The 14-12 spherical motor is composed of a rotor, a stator, a driving electric circuit to generate five-phase ACs (Alternative Currents), and a commercial power supply. Figure 1 shows the composition of the 14-12 spherical motor. The 14-12 spherical motor can rotate around two kinds of axes and totally six axes.

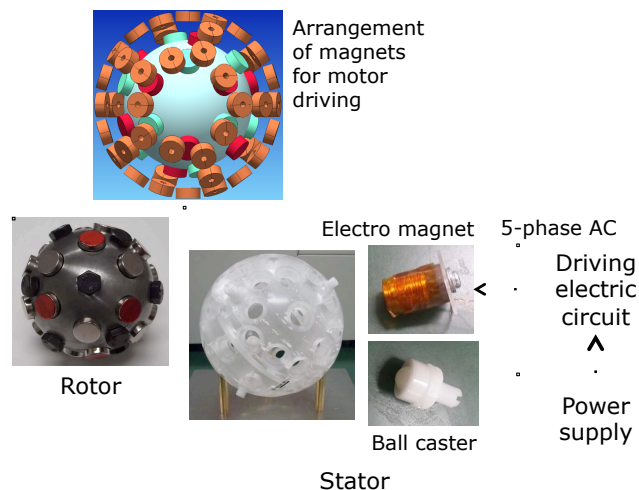


Fig. 1 Composition of 14-12 spherical motor.

B. Rotor and stator

The rotor is an NAK80 spherical shell that is attached with 24 cylindrical NdFeB permanent magnets and 12 iron bolts on its surface and is covered by an acrylic spherical shell. The outer diameter of the rotor is 78 [mm]. The permanent magnets are placed at the vertices of a truncated regular

octahedron inscribed in the outer sphere of the NAK80 spherical shell. On the other hand, iron bolts are placed at the gravity centers of faces of the truncated regular octahedron (square or hexagon) to fix the rotation axis by the attractive force of electro-magnet on the stator.

The stator is composed of an acrylic shell with 62 electro-magnets to generate the rotation force, 6 ball castors to support the rotor, and 3 legs made by brass to place the 14-12 spherical motor on a table. The electro-magnets are placed at the vertices, the midpoints of neighboring two vertices, and the gravity centers of regular pentagon faces of the regular dodecahedron that is inscribed in the inner sphere of the acrylic spherical shell. The ball castors are arranged on the inner surface of the stator to support the rotor with the gap of 4 [mm] from the stator.

C. Rotation axes

The 14-12 spherical motor uses the solid geometry of truncated octahedron and regular dodecahedron for arranging permanent magnets and electro-magnets. Figure 2 shows these solid geometries. Though each face of dodecahedron is regular pentagon, truncated octahedron has two kinds of faces of regular hexagon and square. Therefore, there are two spatial relations between the faces of these solid geometries. According to the two kinds of spatial relations, the 14-12 spherical motor has two rotation axes. They are called as “Axis 1” and “Axis 2” in this study.

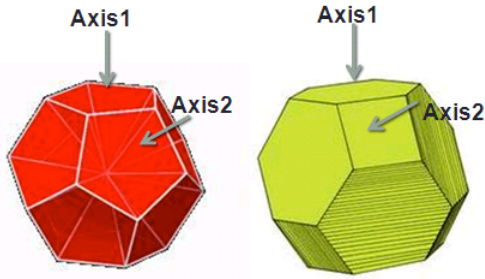


Fig. 2 Regular dodecahedron and truncated octahedron.

III. SIMULATION OF 14-12 SPHERICAL MOTOR

A. Simulation software of magnetic field

This study uses MagNet7 (Infolytica Co.) to simulate dynamic rotation behavior of the 14-12 spherical motor. The MagNet7 is a 2D/3D magnetic field simulation software package. It can model electrical-mechanical devices and solves the Maxwell's equations of magnetic field by the finite element method. It can apply the analyses of transient or time-varying electro-magnetic fields, AC or time harmonic electro-magnetic fields and magneto-static fields with the consideration of motion. Various CAD formats such as DXF, IGES, Inventor (Autodesk Inc.), etc. can be used to represent the geometrical data of an electrical-mechanical device.

B. Simulation model of 14-12 spherical motor

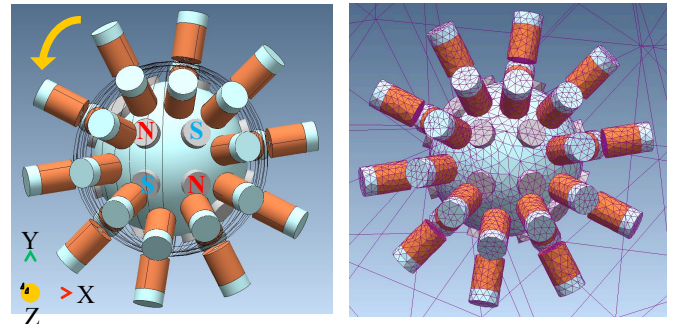
The components of the 14-12 spherical motor modelled are iron spherical shell and permanent magnets of the rotor, electro-magnets composed of fine columnar iron cores with short columnar iron fin at the outer edge and copper wires of

the stator, air gap between the rotor and the stator, and circumferential air. The copper wire of an electro-magnet is modelled as a uniform hollow cylinder of copper equivalent to copper wires of 1000 turns.

This study constructs the geometrical data of the 14-12 spherical motor by the 3D CAD software, Inventor (Autodesk Inc.). The geometrical data are imported to MagNet7 and the materials of electrical and mechanical components are specified as shown in Table 1. The geometrical model of the 14-12 spherical motor is shown in Fig. 3 (a). The frame of reference and rotation direction are also shown in the figure. Calculation meshes generated for the finite element method is shown in Fig. 3 (b). In this study, the maximum element (mesh) size is specified as 2 [mm] for the air gap. The default option that the maximum element size is one tenth of component size is adopted for other components.

Table 1 Components of 14-12 spherical motor modelled and their major material properties and numbers

Component	Material property	Number
Rotor	Iron spherical shell Relative permeability: 1000	1
	Permanent magnet NdFeB Maximum energy product: 48/11 [KJ/m3]	24
Stator	Columnar iron core with fin Relative permeability: 1000	30
	Copper wire Electrical conductivity: 5.77e+7 [S/m]	30
Air gap	Ideal gas	4
Circumferential air	Ideal gas	2



(a) Simulation model

(b) Generated meshes

Fig. 3 Simulation model and generated calculation meshes of 14-12 spherical motor.

C. Simulation cases

The rotation behavior around Axis 2 is simulated for 3000 [ms]. The initial rotation speed is set to 900 [deg/s]. The simulated time corresponds to about eight and half rotations. The air friction and the friction between the rotor and the ball castors usually increase with the increase of rotation speed of the rotor. In this study, the external torque corresponding to them is assumed to be a proportional function of rotation speed. The external torque at the rotation speed of 900 [deg/s] is assumed to be 0.0094 [Nm]. The simulation case is called

Case 1 in this paper. The simulations (Cases 2 to 10) setting constant external torques of 0.01 to 0.05 [Nm] are also conducted for 600 [ms] to investigate the difference of dynamic behavior by the external torque. The conditions of the simulation cases are summarized in Table 2.

Table 2 Simulation cases

Case	Simulation time [ms]	External force
1	3000	Given by a proportion function, 0.0094 [Nm] at 900 [deg/s]
2	600	Constant (0.01 [Nm])
3	600	Constant (0.02 [Nm])
4	600	Constant (0.025 [Nm])
5	600	Constant (0.03 [Nm])
6	600	Constant (0.031 [Nm])
7	600	Constant (0.032 [Nm])
8	600	Constant (0.035 [Nm])
9	600	Constant (0.04 [Nm])
10	600	Constant (0.05 [Nm])

D. Simulation results

The simulated magnetic field before the excitation of electro-magnets by five-phase ACs is shown in Fig. 4. The strength of magnetic field at a point is indicated by color and its direction is shown by a small arrow head. As shown in the figure, the strength of magnetic field is high in the surrounding areas of permanent magnets.

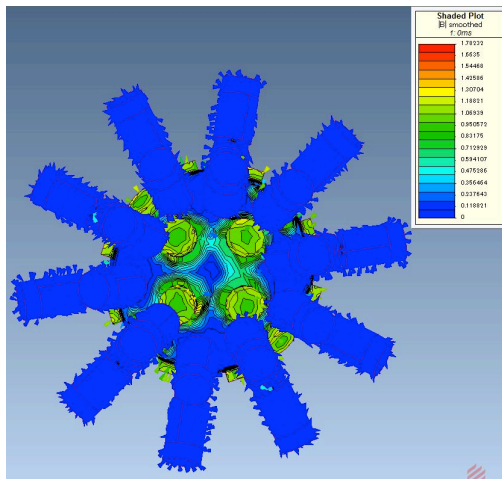


Fig. 4 Simulated magnetic field before exciting electro-magnets.

Table 3 summarizes the continuation of rotation in each case. In the table, the “Y” means that the rotation continues and the “N” means that the rotation stops within 600 [ms]. From the table, the maximum rotation torque at the rotation speed of 900 [deg/s] is estimated as 0.031 [Nm].

Figures 5 shows the time responses of rotation speed and rotation torque in Case 1. Figure 6 shows their time responses in Case 1 for the simulation time period between 2400 and 3000 [ms]. As observed in the figures, there are two types of fluctuations in rotation speed and rotation torque. The one is the major fluctuation. The period of fluctuation is around 400

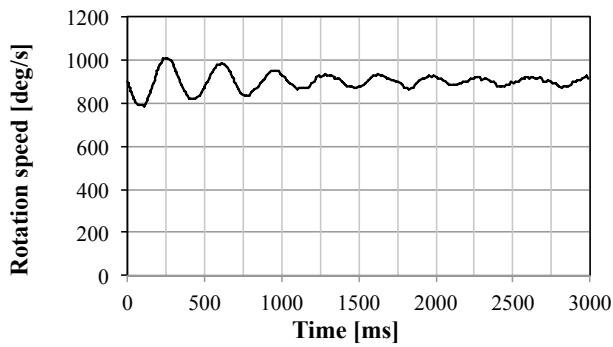
[ms]. The other is the small and fast fluctuation overlapping on the major fluctuation.

Table 3 Simulation results as to the continuation of rotation

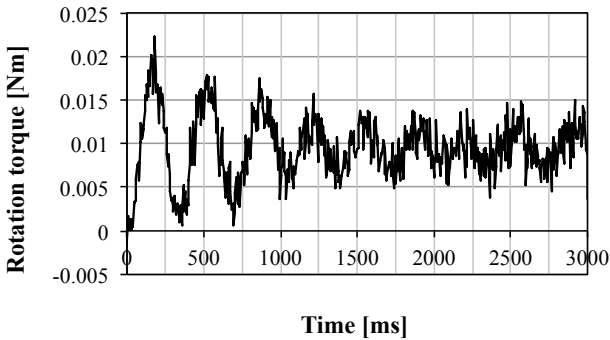
Case	Continuation of rotation
1	Y
2	Y
3	Y
4	Y
5	Y
6	Y
7	N
8	N
9	N
10	N

The period of the major fluctuation seems to converge to 400 [ms] corresponding to the average rotation speed of 900 [deg/s] although it is about 350 [ms] in the initial simulation period. The same tendency is observed in the time response of rotation torque. The average rotation torque is about 0.01 [Nm] that corresponds to the external torque for the average rotation speed of 900 [deg/s]. The amplitudes of major fluctuations decrease according to the convergence. On the contrary, the amplitudes of small and fast fluctuations seem to be almost constant in the whole simulation time. The amplitude of the small and fast fluctuation in the rotation torque is around 0.002 [Nm] as seen from Fig. 6 (b).

The rotation torque is determined by the spatial relations among permanent magnets on the rotor and electro-magnets excited by five-phase ACs. The rotation torque varies because permanent magnets and electro-magnets are arranged on rotor and stator at small intervals. The variation of rotation torque results in varying rotation speed. As seen from Fig. 5 (b), the simulation begins at the rotor posture that almost no rotation torque works. Then, the rotation speed decreases. Although the major fluctuation amplitudes of rotation speed and rotation torque decrease in Case 1, the major fluctuation amplitudes in Case 2 seem not to decrease as shown in Fig. 7. The continuation of the initial major fluctuations in Case 2 may be ascribed to the constant external torque and the phenomenon can be interpreted in the following. In the external torque range that the 14-12 spherical motor can output the rotation torque larger than the external torque, the average output rotation torque will balance the external torque resulting in producing the situation that no external torque works in average. This means that the motor rotates continuously and the major fluctuation of rotation speed preserves. On the other hand, in the case of external torque depending on rotation speed, the external torque at a higher rotation speed than the average rotation speed is larger than that at lower rotation speed. A higher external torque suppresses the increase of rotation speed and a lower external torque suppresses the decrease of rotation speed. In this way, the change of external torque depending on the rotation speed suppresses gradually the amplitudes of major fluctuations of rotation speed and rotation torque.

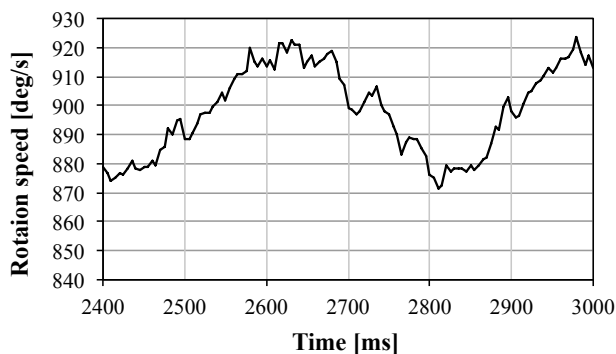


(a) Rotation speed

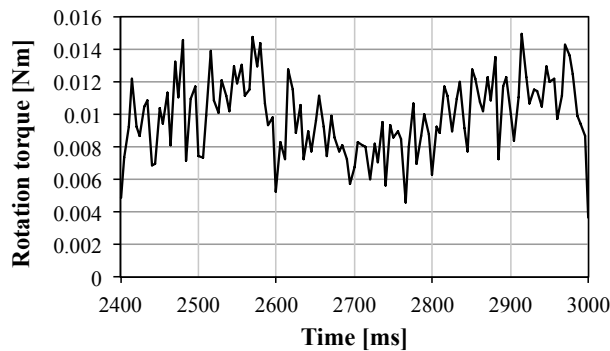


(b) Rotation torque

Fig. 5 Simulated rotation behavior in Case 1.

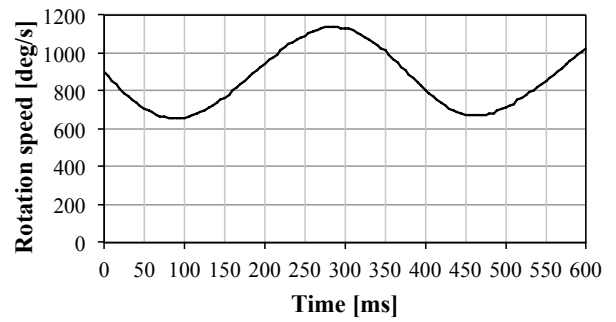


(a) Rotation speed

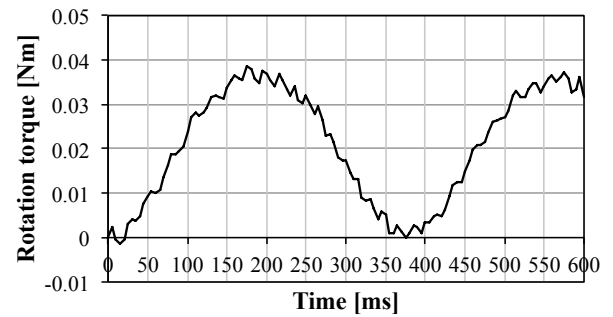


(b) Rotation torque

Fig. 6 Simulated rotation behavior in Case 1 for the simulation time period between 2400 and 3000 [ms].



(a) Rotation speed



(b) Rotation torque

Fig. 7 Simulated rotation behavior in Case 3.

Figure 8 shows the time response of rotation speed in Case 7 that external torque is constant and 0.032 [Nm]. The rotation stops at around 380 [ms] due to the lack of rotation torque. On the other hand, the rotation continues in the cases of constant external torque of not greater than 0.031 [Nm] (Case 6) as shown in Table 3. From the simulation results, the maximum rotation speed at the rotation speed of 900 [deg/s] is estimated as 0.031 [Nm]. However, the results[9] of experimental evaluations show that the output rotation torque around Axis 2 at the rotation speed of 900 [deg/s] is around 0.02 [Nm]. The smaller output rotation torque in the experimental evaluations may be ascribed to the friction loss between the rotor and the ball casters to support the rotor. Further simulations and experimental studies are necessary to investigate the factors to give the difference.

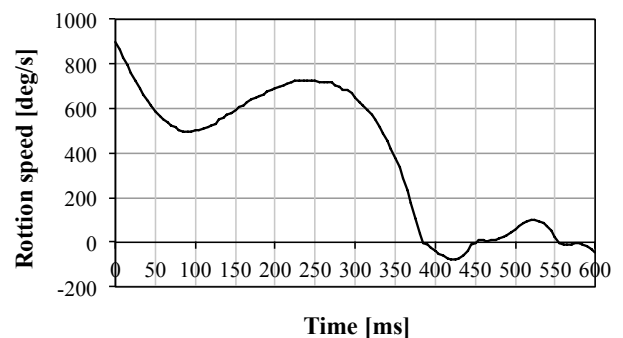


Fig. 8 Simulated time response of rotation speed in Case 7.

The small fluctuations of rotation speed and rotation torque are due to the torque (cogging torque) working between permanent magnets and iron bars of electro-magnets because

the spatial relations between permanent magnets and electro-magnets vary by the rotor rotation. The cogging torque results in the small fluctuations of rotation speed as seen in Figs. 5 (a) and 6 (a). The cogging torque should be zero at the rotation angles when the arrangement of permanent magnets and electro-magnets is symmetric. There are three patterns for the 14-12 spherical motor as shown in Fig. 9. The numbers of symmetric arrangements for the rotations around Axis 1 and 2 are 30 and 40, respectively. In fact, the number of tops and bottoms of the small and fast fluctuations are around 40 for one rotation (400 [ms]) as seen from Fig. 6 (b).

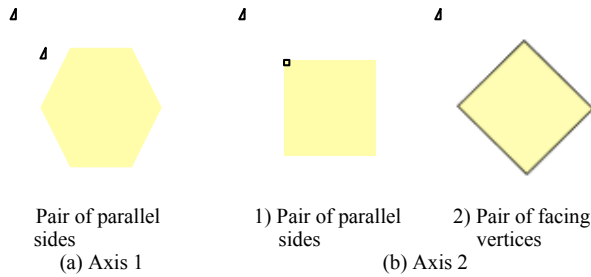


Fig. 9 Patterns of symmetric arrangement of electro-magnets and permanent magnets.

CONCLUSIONS

This study simulates the rotation behaviors of the 14-12 spherical motor in the cases of several load torques. By the simulation results, time changes of rotation speed and rotation torque are confirmed. Small fluctuation is also confirmed to overlap on the time change of rotation torque by the cogging torque.

There are several future topics to be investigated. First, parameter tunings, especially for the specification of material properties are necessary for a more realistic simulation of rotation behavior of the 14-12 spherical motor. Second, several basic rotation performance indexes such as the relation between rotation speed and maximum rotation torque, cogging torque, and so on should be evaluated by simulations. Third, simulation results should be compared with the experimental

results to confirm the applicability of the simulation model developed in this study.

Because numerical simulation is a strong tool to calculate rotation performance of a spherical motor in detail and to search optimum design parameters, the developed simulation model can be used as a base model to design a 14-12 spherical motor having better rotation performance.

REFERENCES

- [1] H. Kanazawa, T. Tsukimoto, T. Maeno, A. Miyake, Tribology of Ultrasonic Motor, *Journal of Japanese Society of Tribologists* (in Japanese), 38 (3), 207-212 (1993).
- [2] B. Dehez, G. Galary, D. Greiner, and B. Raucant : Development of a Spherical Induction Motor With Two Degrees of Freedom, *IEEE Transactions on Magnetics*, 42 (8), 2077-2089 (2006).
- [3] Tomoaki Yano, T. Suzuki, Basic Characteristics of the Small Spherical Stepping Motor, *Proceedings of 2002 IEEE/RSJ International Conference on Intelligent Robots and Systems (IROS'02)*, 1980-1985, (2002).
- [4] Seiji Ikeshita, Akio Gofuku, Tetsushi Kamegawa, Takakazu Nagai, Development of a Spherical Motor Driven by Electro-magnets, *Journal of Mechanical Science and Technology*, 24 (1), 43-46 (2010).
- [5] Wanli Shan, Akio Gofuku, Mitsunobu Shibata, Tomoaki Yano, Tetsushi Kamegawa, A Stirrer Driven by a Spherical Stepping Motor, *Proc. ISEF 2011 - XV International Symposium on Electromagnetic Fields in Mechatronics, Electrical and Electronic Engineering*, (2011).
- [6] Wanli Shan, Akio Gofuku, Tetsushi Kamegawa, Mitsunobu Shibata, Development of a Holonomic Omnidirectional Vehicle Driven by a Spherical Motor and Proposal of a Spherical Deceleration Driving Method, *Transactions of the Japan Society of Mechanical Engineers, Series C*, Vol. 77, No. 784, pp. 4630-4640 (2011). (in Japanese)
- [7] Akio Gofuku, Ryo Sasaki, Tomoaki Yano, Yosuke Wada, Mitsunobu Shibata, Development of a Spherical Stepping Motor Rotating around Six Axes, *Presented in ISEM 2011 - 15th International Symposium on Applied Electromagnetics and Mechanics*, (2011).
- [8] Ryo Sasaki, Akio Gofuku, Tomoaki Yano, Mitsunobu Shibata, Rotation Control of a 14-12 Spherical Stepping Motor, *Proc. the 20th MAGDA Conference in Pacific Asia*, 42-47 (2011).
- [9] Ryo Sasaki, Akio Gofuku, Tomoaki Yano, Mitsunobu Shibata, Basic experimental results of a 14-12 spherical motor, *Proc. Symposium on Power Electronics, Electrical Drives, Automation & Motion*, 832-836, (2012).